Journal of Molecular Catalysis A: Chemical 344 (2011) 74–82

Contents lists available at ScienceDirect

Journal of Molecular Catalysis A: Chemical

journal homepage: www.elsevier.com/locate/molcata

Catalytic behavior and durability of CeO_2 or/and CuO modified USY zeolite catalysts for decomposition of chlorinated volatile organic compounds

Qinqin Huang, Xiaomin Xue, Renxian Zhou*

Institute of catalysis, Zhejiang University, Hangzhou 310028, PR China

ARTICLE INFO

Article history:
Received 19 January 2011
Received in revised form 6 April 2011
Accepted 7 April 2011
Available online 8 May 2011

Keywords:
CuO–CeO_2–USY
CVOCs decomposition
Catalytic behavior
Durability

ABSTRACT

The CeO_2 or/and CuO modified USY zeolite catalysts were prepared and investigated in the catalytic behavior for chlorinated volatile organic compounds (CVOCs) decomposition as well as the durability during 100 h exposure to 1,2-chloroethane (DCE). The results reveal that modified USY catalysts show good catalytic activity for CVOCs decomposition, and high selectivity to the formation of CO_2 and HCl. The better catalytic activity of the CeO_2 or/and CuO modified USY catalysts can be ascribed to the high dispersion of active phases (CeO_2 or CuO), the improved mobility of active oxygen species and the increment of Lewis acidity. The addition of CeO_2 or/and CuO improves the durability of the catalysts during the long term exposure to DCE due to the slight coke deposition and preserved high density of acid sites.

1. Introduction

Chlorinated volatile organic compounds (CVOCs), such as dichloromethane (DCM), 1,2-dichloroethane (DCE), and trichloroethylene (TCE), are a wide-ranging class of solvents commonly found in industrial waste streams and constitute a major source of air and groundwater pollution [1]. Such compounds are well known to be hazardous to the environment and human beings. Some are involved in the depletion of ozone layer as well as the formation of photochemical smog. Some are typically carcinogens, mutagens and teratoges [2,3]. Not only the increasing stringent environmental regulations limiting emissions of CVOCs, but also the increasing amounts of CVOCs released in the environment together with their suspected toxicity and carcinogenic properties, have urged researchers worldwide to find clean and effective methods for destruction of CVOCs. Catalytic oxidation has been considered as a more proper technique for the decomposition of CVOCs compared with direct combustion, due to its less severe conditions (temperature <500 °C), high catalytic performance for the destruction of low concentrations of contaminant (<1000 ppm) and high selectivity to harmless by-products [4,5].

Zeolite is a kind of material with abundant acid sites, especially the Brønsted acidity, which play a key role in the adsorption and destruction of CVOCs [6]. However, easy coke deposition causes the deactivation of zeolites, which inhibits the application in the decomposition of CVOCs [7–10]. In recent years, transition metal (Cr, Mn and Co) modified zeolite catalysts have been studied [11–14]. Those catalysts show good catalytic activity for catalytic oxidation of CVOCs, high selectivity towards the formation of desired products (HCl and CO_2) with less toxicity, and good stability during CVOCs decomposition.

However, less consideration has been given to investigate the suitability of copper modified zeolite catalyst for CVOCs destruction, though it is considered as an effective catalyst for decomposition of non-chlorinated VOCs [15–17]. Abdullah et al. [18] have reported that bimetallic supported H-ZSM-5 ($Cr_{1.0}Cu_{0.5}/SiCl_4$-Z) shows high catalytic activity for decomposition of CVOCs and favorable selectivity to CO_2. Vu et al. [19] have found that $MnCuO_x/TiO_2$ supported catalyst is very active for oxidation of chlorobenzene without formation of any other harmful organic compounds. Moreover, no deactivation of the catalyst is observed. In this paper, we evaluate the catalytic behavior of USY zeolite and cerium or/and copper modified USY zeolite catalysts for the decomposition of various CVOCs (DCM, TCE and DCE). The aim of the present work is to have an investigation of the effect of modification of CeO_2 or/and CuO to USY zeolite on the characteristics, catalytic behavior and durability for CVOCs decomposition.

2. Experimental

2.1. Catalysts preparation

The molar ratio of SiO_2/Al_2O_3 for USY zeolite is 5.3. CeO_2-USY catalyst with CeO_2 loading of 12.5 wt.% was prepared

* Corresponding author. Tel.: +86 571 88273290; fax: +86 571 88273283.
E-mail address: zhourenxian@zju.edu.cn (R. Zhou).

1381-1169/$ – see front matter.
doi:10.1016/j.molcata.2011.04.021

Table 1
Specific surface area and pore volume of USY and modified USY catalysts.

Catalyst	S_{BET} (m^2/g)[a]	V_{Mic} (cm^3/g)[b]	V_{Mes} (cm^3/g)[c]	V_T (cm^3/g)
USY	540.2	0.245	0.141	0.386
CeO_2–USY	468.3	0.211	0.107	0.318
CuO–USY	496.4	0.232	0.130	0.362
CuO–CeO_2–USY	389.3	0.169	0.094	0.263

[a] Calculate from BET method.
[b] Calculated from HK method.
[c] Calculated from BJH method.

by USY impregnated with $Ce(NO_3)_3{\cdot}6H_2O$ (AR, 98.0%) solution. CuO–CeO_2–USY catalyst with CuO and CeO_2 loading of 16.9 and 12.5 wt.% respectively, was prepared by USY zeolite co-impregnated with $Ce(NO_3)_3{\cdot}6H_2O$ and $Cu(NO_3)_3{\cdot}3H_2O$ (AR, 99.5%) solution. The impregnated catalysts were dried at 100 °C for 2 h, then calcined in air at 350 °C for 0.5 h and further at 550 °C for 2 h.

2.2. Catalysts characterization

The nitrogen adsorption–desorption measurement was performed at liquid N_2 temperature on a Coulter ONMISORP-100 apparatus. The catalyst was first degassed under vacuum for 3 h at 200 °C before the measurement.

X-ray diffraction (XRD) measurement was performed on an ARL X'TRA X-ray Diffractometer (Thermo Eelctron Corporation, USA), with Cu Kα radiation at 40 kV and 40 mA in a scanning range of 5–70° (2θ). The XRD analysis of the aged catalyst was performed on the same apparatus and with the same radiation, but in a scanning range of 3–90° (2θ) with a step size of 0.02° and a step time of 2.5 s.

The ammonia temperature-programmed desorption (NH_3-TPD) was performed in a quartz fixed-bed micro-reactor equipped with TCD. Prior to adsorption of ammonia, the catalyst (100 mg) was pretreated in a N_2 stream (99.99%, 35 mL min^{-1}) at 500 °C for 0.5 h. After being cooled down to 100 °C, the catalyst was exposed to a flow (30 mL min^{-1}) of 20 vol.% NH_3/N_2 mixture for 30 min, and then treated in a N_2 flow for 1 h in order to remove physically bound ammonia. Finally, desorption performance was carried out in a N_2 flow (40 mL min^{-1}) from 100 to 600 °C at a heating rate of 10 °C min^{-1}. All these profiles were simulated by Gaussian functions.

The diffuse reflectance infrared spectra of pyridine adsorption (DRIFT) were obtained with a Nicolet Nexus 470 spectrometer (NICOLET Corporation, USA). All spectra were recorded in the range 4000–1300 cm^{-1} with a 2 cm^{-1} resolution. After the catalyst was evacuated at 300 °C at 10^{-5} Torr for 4 h, pyridine vapor was admitted at room temperature until the catalyst surface was saturated. Pyridine was desorbed until a pressure of 10^{-5} Torr to ensure that there was no more physisorbed pyridine. The spectra of adsorbed pyridine were then measured. Different spectra were obtained by subtracting the spectrum of the dehydrated catalysts from the spectra obtained after pyridine adsorption.

The hydrogen temperature-programmed reduction (H_2-TPR) was performed in a quartz fixed-bed micro-reactor equipped with TCD, using a 5 vol.% H_2/Ar mixture. After the catalyst (50 mg) was pretreated in air at 300 °C for 0.5 h, the reduction was carried out from 100 to 800 °C at a heating rate of 10 °C min^{-1}. The H_2 consumption during the reduction was measured by TCD, and the water formed during H_2-TPR was absorbed with 5A molecular sieve.

The coke content of the used catalysts was measured in a Thermogravimetric Analyzer TGA (Perkin Elmer Inc., USA). After the pre-treatment in a N_2 flow (99.99%, 30 mL min^{-1}) at 120 °C for 0.5 h, the used catalyst was further heated up to 800 °C at a rate of 10 °C min^{-1} in a mixture flow (60 mL min^{-1}) of 40 vol.% O_2/N_2.

2.3. Catalytic activity tests

Catalytic activity tests were carried out in a fixed-bed micro-reactor (quartz glass, 6 mm i.d.) at atmospheric pressure. The feed gas (DCE, DCM and TCE) was prepared by delivering the liquid CVOCs by a syringe pump into dry air (dried by silica gel and 5A zeolite), which was metered by a mass flow controller. Its concentration was about 1000 ppm. The gas hourly space velocity (GHSV) was 15,000 h^{-1} with a total flow of 75 mL min^{-1}. The components of gas stream were analyzed by an on-line gas chromatograph equipped with a packed column (OV 101) and a FID detector. Mass spectrum was used for the determination of those detected intermediates (CH_3Cl, C_2H_3Cl, CH_3CHO, CH_3COOH and C_2Cl_4). The conversion was calculated using the area of the $C_2H_4Cl_2$. The amount of CH_3Cl and C_2H_3Cl was calculated from the $C_2H_4Cl_2$ peak. The amount of CH_3CHO, CH_3COOH, C_2HCl_3 and C_2Cl_4 was calculated from the calibration curve of those compounds, respectively.

The temperature-programmed surface reaction (TPSR) measurement was carried out under the catalytic activity tests condition ([DCE] = ~1000 ppm, GHSV = 15,000 h^{-1}) in order to detect the evolutions of the reactant (DCE) and the products (HCl, Cl_2 and CO_2). First, the adsorption of DCE on the catalyst was first carried out at 50 °C. After the adsorption–desorption reached an equilibrium, the catalyst was heated from 50 to 500 °C at a rate of 5 °C min^{-1}. The reactant (DCE) and the products (HCl, Cl_2 and CO_2) were analyzed on-line over a mass spectrometer apparatus (HIDEN QIC-20).

2.4. Durability tests

The durability test of USY and modified USY catalysts was performed under the condition as follows. Each catalyst was exposed to DCE stream ([DCE] = ~1000 ppm) at given temperatures for 100 h. The total flow was 75 mL min^{-1} with GHSV = 15,000 h^{-1}.

3. Results and discussion

3.1. Characterization results

3.1.1. Structure and texture

The specific surface area and pore volume of each catalyst is listed in Table 1. An evident decrease in the specific surface area as well as in the pore volume is observed over modified USY catalysts in comparison with USY zeolite, indicating that those added active phases cause the blockage of the pore channel of USY zeolite. With regard to the loss of pore volume, the decrease is more obvious in the mesopore volume (loss by 24%) than that in micropore volume (loss by 14%) over CeO_2-USY, while the decreases in mesopore volume (loss by 5.3 and 31%) is slightly lower than that in micropore volume (loss by 7.8 and 33%) over CuO–USY and CuO–CeO_2–USY. The results demonstrate that CeO_2 addition mainly causes the reduction in mesopore volume, while CuO addition mainly leads to the decrease in micropore volume. It can be

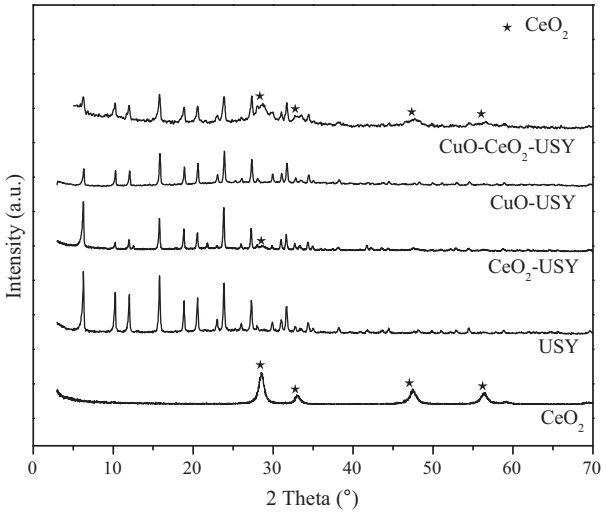

Fig. 1. XRD patterns of CeO_2, USY and modified USY catalysts.

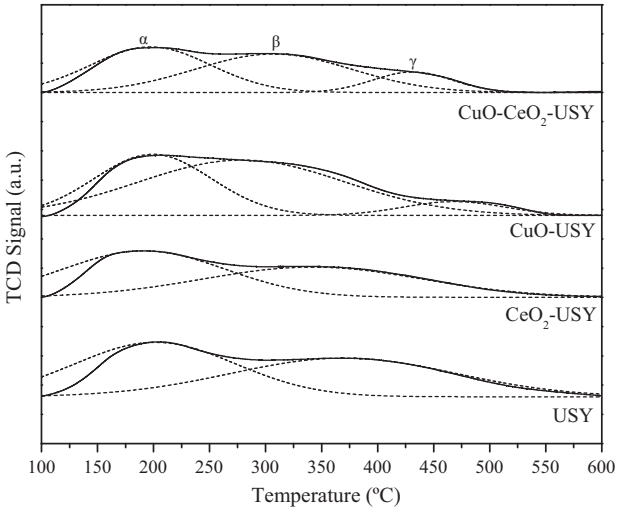

Fig. 2. NH_3-TPD profiles of USY and modified USY catalysts.

due to the smaller radius of Cu^{2+} that can enter the micropore more easily.

The XRD patterns of CeO_2, USY and modified USY catalysts are shown in Fig. 1. For CeO_2–USY, the signals ascribed to fluorite structure ceria (ISCD, No. 28709) are rather weak, indicating high dispersion of CeO_2 on USY zeolite. However, the signal is intense over CuO–CeO_2–USY due to the location of CuO species in the pore channel of USY zeolite hindering the dispersion of CeO_2 species. For CuO–USY and CuO–CeO_2–USY, no distinct diffraction peaks assigned to CuO can be detected over those two catalysts. The results are in agreement with N_2 adsorption/desorption that catalysts with better dispersion of active phases show higher surface area and pore volume. Furthermore, the absence of CuO diffraction peaks in CuO–USY and CuO–CeO_2–USY may be caused by the interaction of CuO with zeolites which results in copper oxide deaggregation and incorporation of single copper ions and/or Cu–O species into the zeolite cationic sites via their exchange with the zeolite bridging OH groups [20]. In addition, the possible formation of CuO–CeO_2 solid solution may occur in CuO–CeO_2–USY [21,22] may also lead to the disappearance of the distinct diffraction peaks of CuO.

3.1.2. Acidity

The NH_3-TPD profiles of USY and modified USY catalysts are shown in Fig. 2. Two distinct desorption peaks are observed over USY and CeO_2–USY. The first peak (peak α) is ascribed to weak acid sites, which shifts to lower temperature range over CeO_2–USY compared with that over USY. The second peak (peak β) is assigned to strong acid sites, which maintains at the similar position for CeO_2–USY as that for USY. In the case of CuO–USY and CuO–CeO_2–USY, the redistribution of the surface acidity is detected. Peak β shifts to lower temperature range, and a third desorption peak (peak γ) with weak intensity is observed at much higher temperature range (>450 °C). The low concentration of this very strong acid site compared with the remaining acid sites are created by the metal cations [13,23,24]. The quantitative analysis is listed in Table 2. We can see that the concentration of total acid sites of the catalysts follows the order of CuO–USY > USY ≫ CuO–CeO_2–USY > CeO_2–USY. Moreover, the percentage of medium strong acidity and strong acidity is higher in CuO–USY and CuO–CeO_2–USY (64.3 and 59.1%, respectively) than that in USY and CeO_2–USY (51.3 and 49.1%, respectively). The results above indicate that the addition of CuO results in the slight decrease in the acidity strength, but leads to the increment in the concentration of acid sites, especially that of medium strong acid sites and strong acid sites.

Table 2
The acidity distribution of USY and modified USY catalysts.

Catalyst	Acidity distribution (mmol NH_3/g)			
	Total	α	β	γ
USY	1.030	0.502	0.527	–
CeO_2–USY	0.750	0.382	0.368	–
CuO–USY	1.036	0.370	0.592	0.074
CuO–CeO_2–USY	0.762	0.312	0.354	0.096

It is well known that diffuse reflectance infrared spectra (DRIFT) of pyridine adsorbed mainly shows the nature of the acid sites, discriminating between Brønsted and Lewis acid sites. The DRIFT spectra of pyridine adsorbed on USY and modified USY catalysts are also determined and shown in Fig. 3. The distinct bands ascribed to Lewis acidity and Brønsted acidity are clearly observed over USY and CeO_2–USY [25,26]. However, the intensity of all the bands is a little weaker on CeO_2–USY compared with that on USY. It is worth noting that the redistribution of the acidity is observed over CuO–CeO_2–USY. The intensity of the bands ascribed to Lewis acidity becomes much more intense while that ascribed to Brønsted

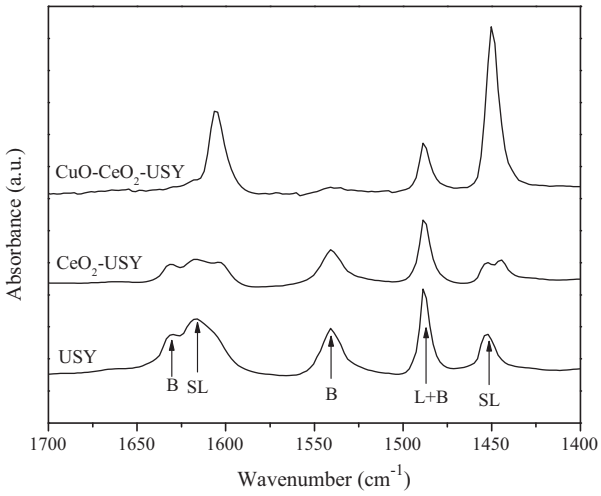

Fig. 3. DRIFT spectra of pyridine adsorbed on USY and modified USY catalysts at 200 °C (SL: strong Lewis acidity, L: Lewis acidity and B: Brønsted acidity).

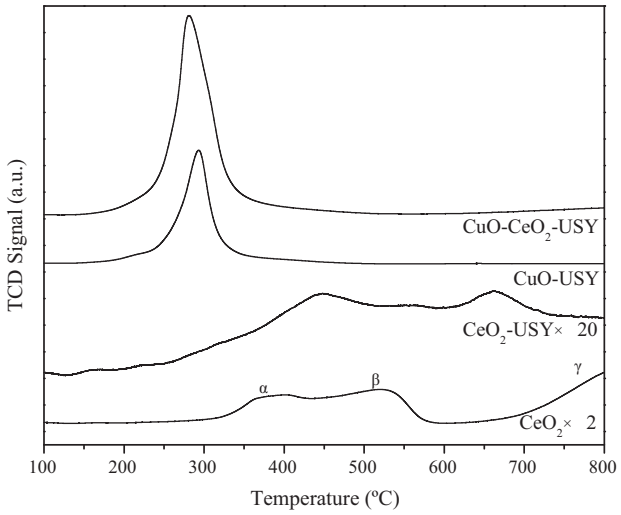

Fig. 4. H_2-TPR profiles of CeO_2 and modified USY catalysts.

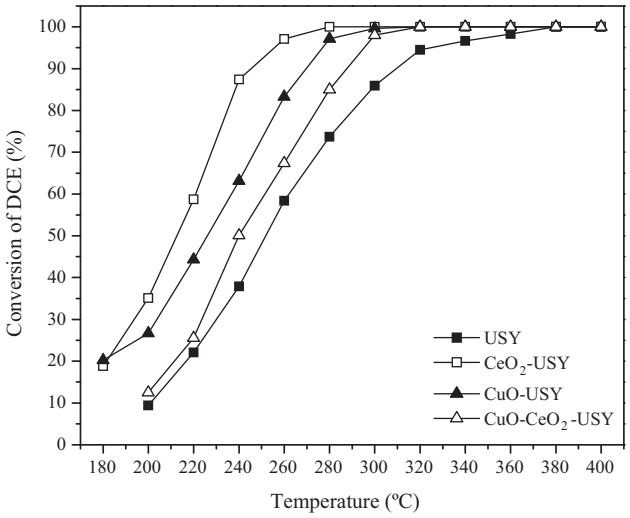

Fig. 5. Conversion of DCE over USY and modified USY catalysts.

acidity is hardly detected. Similar behavior have been observed on modified HZSM-5 zeolite catalysts, which is ascribed to a solid-state reaction between active phases (ZnO, Ge_2O_3 or CuO) and Brønsted acid sites of the zeolite during the preparation and calcination [27–29]. The results are in agreement with NH_3-TPD results. The acidity strength of catalysts is weakened when CuO species are added to USY or CeO_2–USY, since the acidity strength of Lewis acid sites is weaker than that of Brønsted acid sites. Furthermore, the concentration of strong acid sites (strong Lewis acidity) is increased over CuO–CeO_2–USY compared with that over CeO_2–USY as observed from NH_3-TPD results.

3.1.3. Redox property

The temperature-programmed reduction technique is a conventional method for characterizing the reducibility of the catalysts. The H_2-TPR profiles of the catalysts are shown in Fig. 4. Evidently, three reduction peaks are observed on pure CeO_2. Peaks α and β detected below 600 °C are ascribed to the reduction of surface and sub-surface oxygen, and peak γ observed above 600 °C is assigned to the reduction of bulk oxygen [30]. When CeO_2 species are loaded on USY zeolite, the reduction peaks of both surface oxygen and bulk oxygen evidently shift to lower temperature range, indicating the good mobility of the oxygen species. Moreover, the broad peak observed within the temperature 250–600 °C also demonstrates the good redox property of CeO_2–USY [31,32]. There is only one reduction peak with high intensity detected over CuO contained catalysts. The peak temperature of the reduction peak is 293 and 282 °C over CuO–USY and CuO–CeO_2–USY, respectively. It is noticeable that not only the peak temperature of the reduction peak shifts to lower temperature, but the intensity of the reduction peak is enhanced for CuO–CeO_2–USY compared with that for CuO–USY. The results indicate that the reduction of CuO species is promoted by cerium addition via the strong interaction between CuO and CeO_2 species [33].

3.2. Catalytic activity results

The catalytic activity for the decomposition of DCE over USY and modified USY catalysts is presented in Figs. 5 and 6. As shown in Fig. 5, the catalytic activity for DCE decomposition, based on T_{90} (temperature at which 90% conversion is attained), decreases in the following order of CeO_2–USY(246 °C) > CuO–USY(269 °C) > CuO–CeO_2–USY(288 °C) > USY(310 °C). The results indicate that the addition of CeO_2 or/CuO to USY zeolite results in the interaction between active phases and USY zeolite, which shows an evident enhancement in decomposition of DCE.

The concentration–temperature relationships of major by-products CH_3Cl, C_2H_3Cl, CH_3CHO and CH_3COOH during DCE decomposition are presented in Fig. 6. Large concentration of CH_3Cl and C_2H_3Cl are produced over USY zeolite, but nearly no CH_3CHO or CH_3COOH is detected. When CeO_2 is introduced to USY zeolite, the concentration of CH_3Cl is decreased due to the decrease in strong acid sites. However, the concentration of C_2H_3Cl, CH_3CHO and CH_3COOH is increased, with the maximum value observed at 320, 360, and 360 °C, respectively. The results indicate that the interaction between CeO_2 species and USY zeolite is beneficial to the dehydrochlorination of DCE [34,35]. However, the decrease in protonic acid sites (strong acid sites) in CeO_2–USY compared with that in USY inhibits the further dehydrochlorination process of C_2H_3Cl, thus, the concentration of C_2H_3Cl is higher over CeO_2–USY than that over USY. At the same time, the presence of active oxygen species over CeO_2–USY promotes the production of CH_3CHO and CH_3COOH. In addition, small amount of $C_2H_2Cl_2$ (always <20 ppm) is detected over USY and CeO_2–USY (not shown in Fig. 6), which may be resulted from the chlorination of C_2H_3Cl followed by dehydrochlorination [30,31,36]. It is noticeable that the concentration of CH_3Cl and C_2H_3Cl is obviously decreased over CuO–USY and CuO–CeO_2–USY. However, a certain amount of high chlorinated by-products C_2HCl_3 and C_2Cl_4 is detected (not shown in Fig. 6). The production of high chlorinated by-products during CVOCs catalytic decomposition over Cu-based catalysts has been reported by other researchers [37]. We deduce that C_2HCl_3 may be formed through chlorination of $C_2H_2Cl_2$ followed by dehydrochlorination due to the presence of CuO species, while C_2Cl_4 may be formed via the chlorination of C_2HCl_3 followed by dehydrochlorination. The production of CH_3CHO and CH_3COOH is obviously promoted at lower temperature range with CuO added to USY or CeO_2–USY, due to the abundant amount of active oxygen species with better mobility in the catalysts as stated in the results of redox property.

The adsorption–desorption behavior of DCE and the evolutions of the main products (CO_2, HCl and Cl_2) over the catalysts have been further investigated by TPSR technique, in order to evaluate the selectivity towards the formation of HCl and CO_2. As presented in Fig. 7, desorption of DCE occurs at relatively low temperature range accompanied with DCE decomposition. When CeO_2 or CuO is introduced into USY, the intensity of desorption peak is enhanced and the peak-temperature of desorption peak shifts to higher tem-

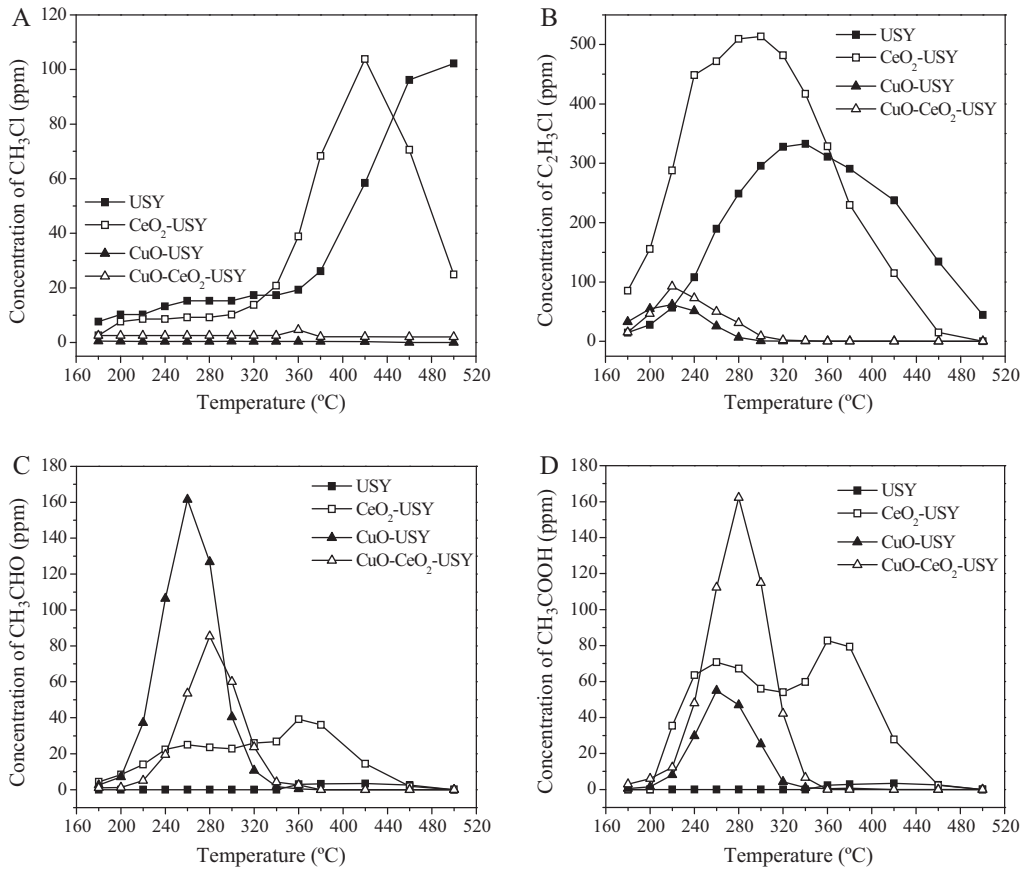

Fig. 6. Concentration–temperature relation of the by-products during DCE decomposition over USY and modified USY catalysts: (A) CH_3Cl, (B) C_2H_3Cl, (C) CH_3CHO and (D) CH_3COOH.

perature range. It indicates that the synergy between active phases (CeO_2 and CuO) and USY zeolite is of great significance to improve the integration of adsorption–desorption-catalysis process. The peak is weakened and broadened with the peak-temperature further shifting to higher temperature range over CuO–CeO_2–USY. It is speculated that much stronger adsorption of DCE occurs on CuO–CeO_2–USY, which inhibits desorption and decomposition of DCE to some extent.

In the case of CO_2 evolution, CO_2 is observed at the temperature as low as 250 °C over modified USY catalysts, while CO_2 can

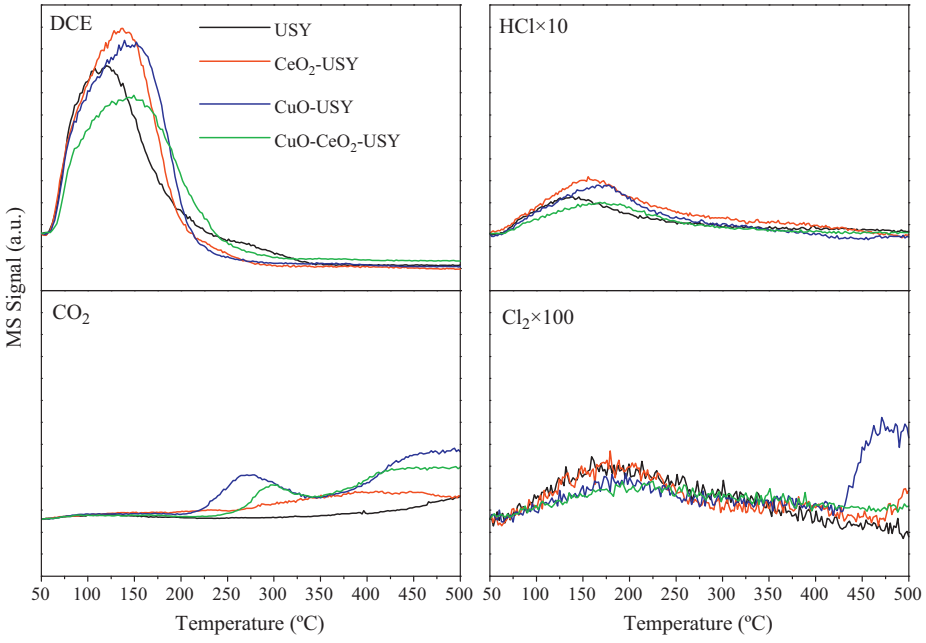

Fig. 7. TPSR profiles for DCE decomposition over modified USY catalysts.

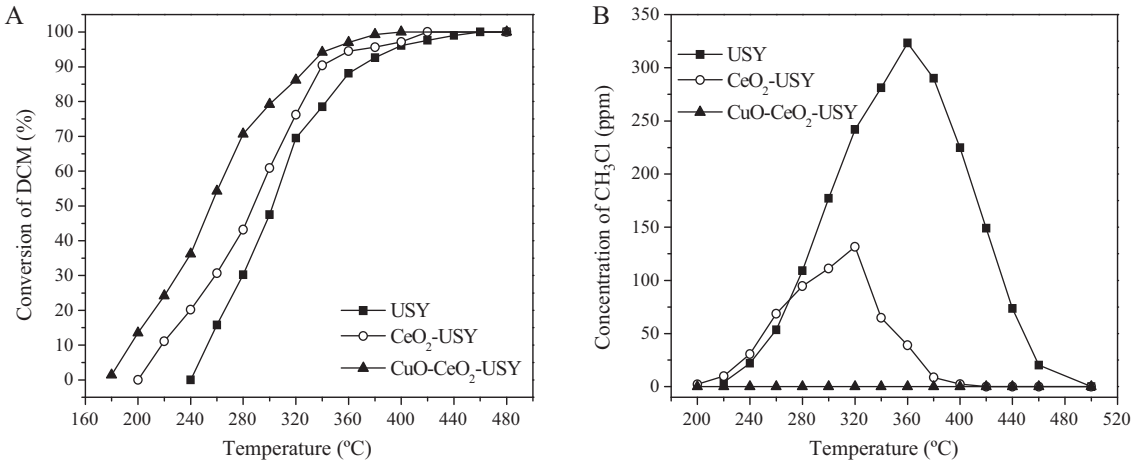

Fig. 8. Catalytic activity for DCM decomposition over USY and modified USY catalysts: (A) conversion of DCM and (B) concentration of CH_3Cl.

only be detected until the temperature reaches 400 °C over USY. It indicates that the synergy between active phases and USY zeolite promotes the selectivity to the formation of CO_2. It is interesting to note that one more peak is observed below 350 °C over CuO–USY and CuO–CeO_2–USY, which may be ascribed to a combined signal of CO_2 produced during DCE decomposition and the desorption of CO_2 adsorbed at low temperatures on the catalysts [38]. The sequence of the selectivity to CO_2 over these catalysts is as follows: CuO–USY > CuO–CeO_2–USY > CeO_2–USY > USY. Based on the mechanism of DCE decomposition, the pathway of the CO_2 produced over each catalyst is different. For modified USY catalysts, the production of CO_2 can be assigned to the further oxidation of acetate species in the presence of active oxygen species [35]. For USY zeolite, the increment of CO_2 within high temperature range may be resulted from the oxidation of coke deposited on the surface of USY zeolite.

The evolutions of HCl and Cl_2 demonstrate that HCl is the major chlorinated by-product within the temperature range 50–400 °C, which is a preferred chlorinated product instead of Cl_2. The results can be ascribed to the two reasons presented below. (i) DCE contains sufficient hydrogen atoms for the complete oxidation to the desired products [6]. (ii) The hydroxyls in the zeolites structure largely promote HCl formation by the Deacon reaction ($2HCl + 1/2O_2 \leftrightarrow Cl_2 + H_2O$), especially in the combustion of compounds with a low H/Cl ratio [39,40]. As the temperature further increases, the amount of Cl_2 shows an increase over CeO_2–USY and CuO–USY. It can be explained as the fact that the oxidation of HCl is promoted at higher temperature range according to Deacon reaction in the presence of active oxygen species [35,39]. However, the amount of Cl_2 remains stable over CuO–CeO_2–USY. It may be due to the interaction between CuO and CeO_2 that inhibits the increase of Cl_2 production.

On the basis of the results above, USY, CeO_2–USY and CuO–CeO_2–USY are chosen for decomposition of DCM and TCE in order to have a further investigation of the effect of interaction between CuO and CeO_2 on the catalytic behavior of the catalysts. The catalytic activity for DCM and TCE decomposition over USY and modified USY catalysts is presented in Figs. 8 and 9, respectively.

We can see from Fig. 8(A) that DCM can be completely converted within 450 °C over USY. With the introduction of CeO_2 or/and CuO species, the conversion for DCM decomposition is improved. Based on T_{90}, the catalytic activity of the catalysts decreases in the following order of CuO–CeO_2–USY(330 °C) > CeO_2–USY(340 °C) > USY(370 °C). CH_3Cl is the main by-product during DCM decomposition. As shown in Fig. 8(B), large concentration of CH_3Cl is produced over USY and the maximum value is observed at about 360 °C, which is closed to the temperature of complete conversion of DCM. It is noticeable that the concentration of CH_3Cl is decreased evidently over modified USY catalysts, especially over CuO–CeO_2–USY that CH_3Cl can no longer be detected within the whole temperature. The results indicate that the addition of active phases shows

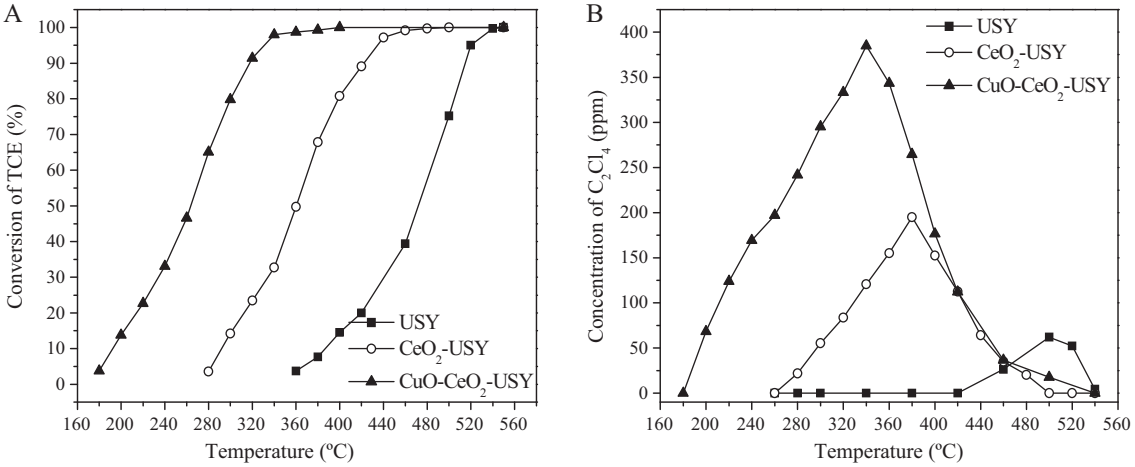

Fig. 9. Catalytic activity for TCE decomposition over USY and modified USY catalysts: (A) conversion of TCE and (B) concentration of C_2Cl_4.

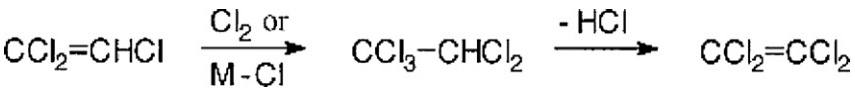

Fig. 10. The mechanism of the formation of C_2Cl_4 during TCE decomposition.

obvious limitation on the production of CH_3Cl, which is beneficial to the oxidation of DCM into CO_x and HCl [39,41]. According to the findings reported by Brink et al. [41], DCM first reacts with surface hydroxyl groups resulting adsorbed formaldehyde intermediates and HCl. Then, the formaldehyde disproportionates into methoxy and formate species. The former further converts to CO_x and the latter can react with HCl to form the main by-product methylchloride. In our study, as a result, the improved catalytic activity of modified USY catalysts for DCM decomposition may be related to the co-existence of both acidity and better mobility of oxygen species in the catalysts as revealed in the results of acidity and redox property. Moreover, the presence of active oxygen species in modified USY catalysts promotes the HCl consumption via Deacon reaction. Therefore, the formation of CH_3Cl is decreased through the reaction of methoxy with HCl. Especially over CuO–CeO_2–USY, no CH_3Cl is detected due to the much better mobility of oxygen species as stated in the results of redox property.

We can see from Fig. 9 that the addition of CeO_2 or/and CuO species to USY evidently enhances the catalytic activity for TCE decomposition. On the basis of T_{90}, the catalytic activity of the catalysts follows the order: CuO–CeO_2–USY(318 °C) > CeO_2–USY(422 °C) > USY(515 °C). C_2Cl_4 is the main by-product during TCE decomposition. Small concentration of C_2Cl_4 is produced over USY. However, the production of C_2Cl_4 is evidently increased over modified USY catalysts. Especially over CuO–CeO_2–USY, large concentration of C_2Cl_4 is detected with the maximum value observed at about 340 °C. However, the by-product can be completely decomposed at high temperatures (<500 °C). According to the mechanism of TCE decomposition, it is deduced that TCE first decomposes on acid sites with the evolution of HCl and CO_x [34,42]. And the formation of C_2Cl_4 is resulted from the chlorination of TCE followed by dehydrochlorination in the presence of noble metals and metal oxides as exhibited in Fig. 10 [34,43]. Due to the promoted formation of Cl_2 via Deacon reaction over modified USY catalysts with active oxygen species as stated in the results of redox property, the reaction between TCE and Cl_2 to yield C_2Cl_4 is enhanced. At the same time, the catalytic activity for TCE decomposition is also improved, especially over CuO–CeO_2–USY.

3.3. Durability of USY and modified USY catalysts

The catalytic durability of the catalysts in the decomposition of DCE as conversion vs. time on stream is presented in Fig. 11. As shown in Fig. 11(A), the conversion falls rapidly in the initial stages of the reaction and decreases from 87 to 27% over USY after 100 h tests, while the conversion maintains at 100% over modified USY catalysts. However, it is known that a certain part of the catalyst bed may not participate in the reaction when the conversion reaches 100%. Therefore, we re-evaluated the durability of CeO_2–USY and CuO–CeO_2–USY under relatively low conversions. As shown in Fig. 11(B), DCE conversion falls from 88 to 63% in the first 40 h over CeO_2–USY and stays at 60% in the rest time, while it falls from 85 to 72% in the initial 20 h and maintains at about 70% during the rest reaction time. The results indicate that the modification to the USY zeolite evidently enhances the durability of the catalysts during the long term tests. Especially for CuO–CeO_2–USY that the interaction between CeO_2 and CuO further improves the durability of the catalyst.

It is well known that coke deposition easily takes place on zeolite [10,44]. As listed in Table 3, severe coke deposition is observed in USY while much lower coke content is detected over the modified USY catalysts. It indicates that the presence of abundant oxygen species, which is in favor of the deeper oxidation of DCE into CO_2, inhibits the production of coke during the long time reaction. Therefore, the rather slight coke deposition over modified USY catalysts is one of the factors to the good durability during the long time tests.

With regard to the acidity of the aged catalysts, both USY-A and CeO_2–USY-A catalysts show the loss of the total acidity, which is more evident for the former compared with that for the latter. Interestingly, the increase in the total acidity is observed over CuO–CeO_2–USY-A. It may be related to the complete change in the zeolite framework of the catalyst, which will be discussed below. The preserved relatively high density of acid sites may be another factor to the high conversion of DCE maintained during the long time tests.

The XRD analysis of the used catalysts is carried out in order to determine the change in the zeolite framework. As shown in Fig. 12, it is observed that USY-A and CeO_2–USY-A preserve

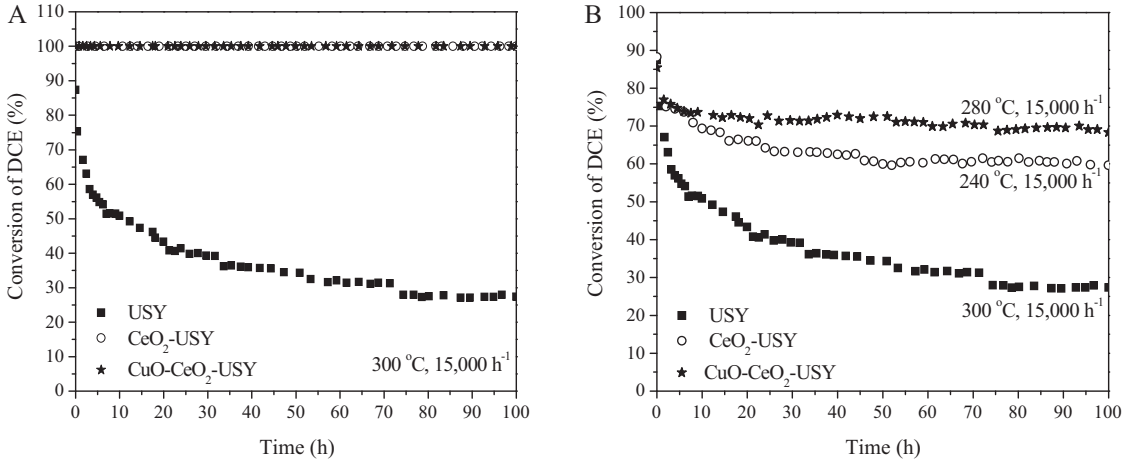

Fig. 11. The conversion of DCE over USY, CeO_2–USY and CuO–CeO_2–USY as a function of time on stream: (A) at 300 °C and (B) at various temperatures.

Table 3
Coke content, total acidity and crystallinity of the catalysts after 100 h tests (300 °C, 15,000 h^{-1}).

	Coke content (%)	Total acidity (mmol NH_3/g) (used/fresh)	Crystallinity (%)
USY-A[a]	11.4	0.589/1.030	90.0
CeO_2–USY-A	1.1	0.617/0.750	84.1
CuO–CeO_2–USY-A	1.5	1.035/0.762	95.8

[a] Catalysts after 100 h test.

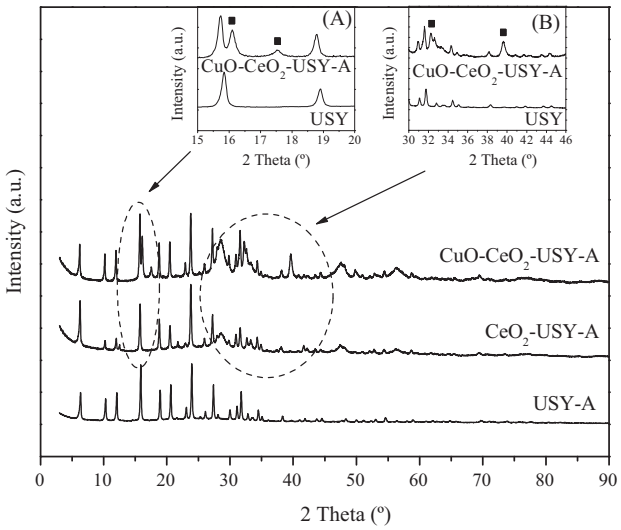

Fig. 12. XRD patterns of the catalysts after 100 h test (inset figures: XRD patterns of fresh USY and CuO–CeO_2–USY-A from 15° to 20° (A) and 30° to 46° (B)).

the same framework of USY zeolite (space group *Fd*3*m*), and the crystallinity is 90.0% and 84.1% for USY-A and CeO_2–USY-A, respectively (listed in Table 3), indicating the relatively good structure stability during long time tests. It is worth noting that new diffraction peaks ascribed to the space group (*Fm*3*m*) are observed over CuO–CeO_2–USY-A compared with fresh USY zeolite (shown in the inset figures of Fig. 12). Meanwhile, the total acidity increase obviously compared with that of USY-A (Table 3). Such changes may be related to the stimulated migration of Cu species into the zeolite bulk by coordination of copper ions to water molecules produced during DCE decomposition [20]. However, the change in the zeolite structure does not show negative effect on the catalytic activity for DCE decomposition. In addition, the crystallinity of CuO–CeO_2–USY-A shows an evident increase compared with that of fresh USY zeolite during the long time exposure to DCE, which also demonstrate the good stability of CuO–CeO_2–USY.

4. Conclusions

The CeO_2 or/and CuO modified USY zeolite catalysts were prepared by impregnation method and investigated in the catalytic behavior for decomposition of CVOCs as well as the stability during long exposure to DCE. All the catalysts were characterized by means of N_2 adsorption–desorption, XRD, NH_3-TPD, DRIFT and H_2-TPR. The results reveal that CeO_2–USY shows the best catalytic activity for DCE decomposition, and CuO–CeO_2–USY presents the highest catalytic activity for the decomposition of DCM and TCE. The better catalytic activity of modified USY catalysts for CVOCs decomposition can be ascribed to the high dispersion of active CeO_2 or CuO species, the limited formation of CuO–CeO_2 solid solution over CuO–CeO_2–USY, the improved mobility of active oxygen species and the increment of Lewis acidity. Due to the presence of abundant active oxygen species with better mobility and stronger oxidizability over modified USY catalysts, the production of CH_3CHO and CH_3COOH is promoted and the production of CH_3Cl and C_2H_3Cl is inhibited. The high selectivity to the formation of HCl and CO_2 over modified USY catalysts can be attributed to the existence of abundant hydroxyls groups and active oxygen species. The addition of CeO_2 or/and CuO to USY zeolite improves the durability of the catalysts with slight coke deposition and relatively high density of acid sites over used catalysts.

Acknowledgements

We gratefully acknowledge the financial supports from the Ministry of Science and Technology of China (No. 2011AA03A406).

References

[1] E.C. Moretti, Practical Solutions for Reducing Volatile Organic Compounds and Hazardous Air Pollutants, Center for Waste Reduction Technologies of the American Institute of Chemical Engineers, New York, 2001.
[2] A. Aranzabal, J.A. González-Marcos, J.L. Ayastuy, J.R. González-Velasco, Chem. Eng. Sci. 61 (2006) 3564–3576.
[3] R. López-Fonseca, A. Aranzabal, P. Steltenpohl, J.I. Gutiérrez-Ortiz, J.R. González-Velasco, Catal. Today 62 (2000) 367–377.
[4] J.R. González-Velasco, A. Aranzabal, J.I. Gutiérrez-Ortiz, R. López-Fonseca, M.A. Gutiérrez-Oritiz, Appl. Catal. B: Environ. 19 (1998) 189–197.
[5] P. Hunter, S.T. Oyama, Control of Volatile Organic Compounds Emissions: Conventional and Emerging Technologies, Wiley-Interscience, New York, 2000.
[6] R. López-Fonseca, J.I. Gutiérrez-Oritz, M.A. Gutiérrez-Ortiz, J.R. González-Velasco, J. Catal. 209 (2002) 145–150.
[7] M. Tajima, M. Niwa, Y. Fujii, Y. Koinuma, R. Aizawa, S. Kushiyama, S. Kobayashi, K. Mizuno, H. Ohûchi, Appl. Catal. B: Environ. 9 (1996) 167–177.
[8] J.R. González-Velasco, R. López-Fonseca, A. Aranzabal, J.I. Gutiérrez-Ortiz, P. Steltenpohl, Appl. Catal. B: Environ. 24 (2000) 233–242.
[9] L. Intriago, E. Díaz, S. Ordóñez, A. Vega, Micropor. Mesopor. Mater. 91 (2006) 161–169.
[10] A. Aranzabal, J.A. González-Marcos, M. Romero-Sáez, J.R. González-Velasco, Appl. Catal. B: Environ. 88 (2009) 533–541.
[11] G.A. Atwood, H.L. Greene, P. Chintawar, R. Rahcapudi, B. Ramachandran, C.A. Vogel, Appl. Catal. B: Environ. 18 (1998) 51–61.
[12] S. Kawi, M. Te, Catal. Today 44 (1998) 101–109.
[13] J.I. Gutiérrez-Ortiz, R. López-Fonseca, U. Aurrekoetxea, J.R. González-Velasco, J. Catal. 218 (2003) 148–154.
[14] P.S. Chintawar, H.L. Greene, Appl. Catal. B: Environ. 13 (1997) 81–92.
[15] M.F. Ribeiro, J.M. Silva, S. Brimaud, A.P. Antunes, E.R. Silva, A. Fernandes, P. Magnoux, D.M. Murphy, Appl. Catal. B: Environ. 70 (2007) 384–392.
[16] W.B. Li, M. Zhuang, J.X. Wang, Catal. Today 137 (2008) 340–344.
[17] M. Karthik, L.-Y. Lin, H. Bai, Micropor. Mesopor. Mater. 117 (2009) 153–160.
[18] A.Z. Abdullah, M.Z.A. Bakar, S. Bhatia, J. Hazard. Mater. B129 (2006) 39–49.
[19] Van Hinh Vu, Jamal Belkouch, Aïssa Ould-Dris, Bechara Taouk, J. Hazard. Mater. 169 (2009) 758–765.
[20] B. Wichterlová, Z. Sobalík, M. Skokánek, Appl. Catal. A: Gen. 103 (1993) 269–280.
[21] P. Djinović, J. Batista, A. Pintar, Appl. Catal. A: Gen. 347 (2008) 23–33.
[22] M. Schmal, C.A. Perez, V.T. da Silva, L.F. Padilha, Appl. Catal. A: Gen. 375 (2010) 205–212.
[23] B. Wichterlova, S. Beran, S. Bednarova, K. Nedomova, L. Dudikova, P. Jiru, Stud. Surf. Sci. Catal. 37 (1988) 199–206.
[24] D.J. Parrillo, C. Pereira, G.T. Kokotailo, R.J. Gorte, J. Catal. 138 (1992) 377–385.
[25] B. Chakraborty, B. Viswanathan, Catal. Today 49 (1999) 253–260.
[26] T. Barzetti, E. Salli, D. Moscotti, L. Forni, J. Chem. Soc., Faraday Trans. 92 (1996) 1401–1407.
[27] V.I. Yakerson, T.V. Vasina, L.I. Lafer, V.P. Sytnyk, G.L. Dykh, A.V. Mokhov, O.V. Bragin, K.M. Minachev, Catal. Lett. 3 (1989) 339–345.
[28] C.C. Salguero, Y.L. Lam, M. Schmal, Catal. Lett. 47 (1997) 143–154.
[29] M.H.O. Nunes, V. Teixeira da Silva, M. Schmal, Appl. Catal. A: Gen. 294 (2005) 148–155.
[30] J.M. Zhou, L. Zhao, Q.Q. Huang, R.X. Zhou, X.K. Li, Catal. Lett. 127 (2009) 277–284.
[31] Q.Q. Huang, X.M. Xue, R.X. Zhou, J. Mol. Catal. A: Chem. 331 (2010) 130–136.
[32] Y. Guo, G.Z. Lu, Z.G. Zhang, S.H. Zhang, Y. Qi, Y. Liu, Catal. Today 126 (2007) 296–302.
[33] T. Caputo, L. Lisi, R. Pirone, G. Russo, Appl. Catal. A: Gen. 348 (2008) 42–53.
[34] M.M.R. Feijen-Jeurissen, J.J. Jorna, B.E. Nieuwenhuys, G. Sinquin, C. Petit, J.-P. Hindermann, Catal. Today 54 (1999) 65–79.

[35] B. de Rivas, R. López-Fonseca, J.R. González-Velasco, J.I. Gutiérrez-Ortiz, J. Mol. Catal. A: Chem. 278 (2007) 181–188.
[36] Q.Q. Huang, X.M. Xue, R.X. Zhou, J. Hazard. Mater. 183 (2010) 694–700.
[37] Chul-Hoon Cho, Son-Ki Ihm, Environ. Sci. Technol. 36 (2002) 1600–1606.
[38] Z.X. Yang, B.L. He, Z.S. Lu, K. Hermansson, J. Phys. Chem. C 114 (2010) 4486–4494.
[39] B. Ramachandran, H.L. Greene, S. Chatterjee, Appl. Catal. B: Environ. 8 (1996) 157–182.
[40] H.L. Greene, D.S. Prakash, K.V. Athota, Appl. Catal. B: Environ. 7 (1996) 213–224.
[41] R.W. van den Brink, P. Mulder, R. Louw, G. Sinquin, C. Petit, J.-P. Hindermann, J. Catal. 180 (1998) 153–160.
[42] B. de Rivas, R. López-Fonseca, J.R. González-Velasco, J.I. Gutiérrez-Ortiz, Catal. Commun. 9 (2008) 2018–2021.
[43] J.I. Gutiérrez-Ortiz, B. de Rivas, R. López-Fonseca, J.R. González-Velasco, Appl. Catal. A: Gen. 269 (2004) 147–155.
[44] S. Chatterjee, H.L. Greene, Y.J. Park, Catal. Today 11 (1992) 569–596.